



HAL
open science

Early fungi from the Proterozoic era in Arctic Canada

Corentin C. Loron, Camille François, Robert H. Rainbird, Elizabeth C. Turner,
Stephan Borensztajn, Emmanuelle J. Javaux

► To cite this version:

Corentin C. Loron, Camille François, Robert H. Rainbird, Elizabeth C. Turner, Stephan Borensztajn, et al.. Early fungi from the Proterozoic era in Arctic Canada. *Nature*, 2019, 570, pp.232-235. <10.1038/s41586-019-1217-0>. <insu-03586648>

HAL Id: insu-03586648

<https://insu.hal.science/insu-03586648v1>

Submitted on 7 Oct 2025

HAL is a multi-disciplinary open access archive for the deposit and dissemination of scientific research documents, whether they are published or not. The documents may come from teaching and research institutions in France or abroad, or from public or private research centers.

L'archive ouverte pluridisciplinaire HAL, est destinée au dépôt et à la diffusion de documents scientifiques de niveau recherche, publiés ou non, émanant des établissements d'enseignement et de recherche français ou étrangers, des laboratoires publics ou privés.



Distributed under a Creative Commons CC BY 4.0 - Attribution - International License

Early fungi from the Proterozoic era in Arctic Canada

Corentin C. Loron^{1*}, Camille François¹, Robert H. Rainbird², Elizabeth C. Turner³, Stephan Borensztajn⁴ & Emmanuelle J. Javaux^{1*}

Fungi are crucial components of modern ecosystems. They may have had an important role in the colonization of land by eukaryotes, and in the appearance and success of land plants and metazoans^{1–3}. Nevertheless, fossils that can unambiguously be identified as fungi are absent from the fossil record until the middle of the Palaeozoic era^{4,5}. Here we show, using morphological, ultrastructural and spectroscopic analyses, that multicellular organic-walled microfossils preserved in shale of the Grassy Bay Formation (Shaler Supergroup, Arctic Canada), which dates to approximately 1,010–890 million years ago, have a fungal affinity. These microfossils are more than half a billion years older than previously reported unambiguous occurrences of fungi, a date which is consistent with data from molecular clocks for the emergence of this clade^{6,7}. In extending the fossil record of the fungi, this finding also pushes back the minimum date for the appearance of eukaryotic

crown group Opisthokonta, which comprises metazoans, fungi and their protist relatives^{8,9}.

Several Precambrian microfossils have been tentatively interpreted as fungi in the past fifty years¹⁰ (for further examples and specimen names, see Supplementary Information). A few Proterozoic fossils—notably, parts of the Ediacaran biota—have been compared to lichen-like organisms¹¹. All of these previous studies have focused on broad morphological comparisons; in isolation, this methodology cannot fully support a specific affiliation with the fungi⁴. Nevertheless, when combined with the acetolysis resistance of chemically recalcitrant structures that have been tested in several fungal lineages¹², the Palaeozoic record^{4,5} indicates that fungi have a strong potential for preservation in the geological record. To conclusively identify fungal or other eukaryotic fossils, morphological evidence needs to be coupled with analyses of the ultrastructure and chemical composition of microfossils¹³.

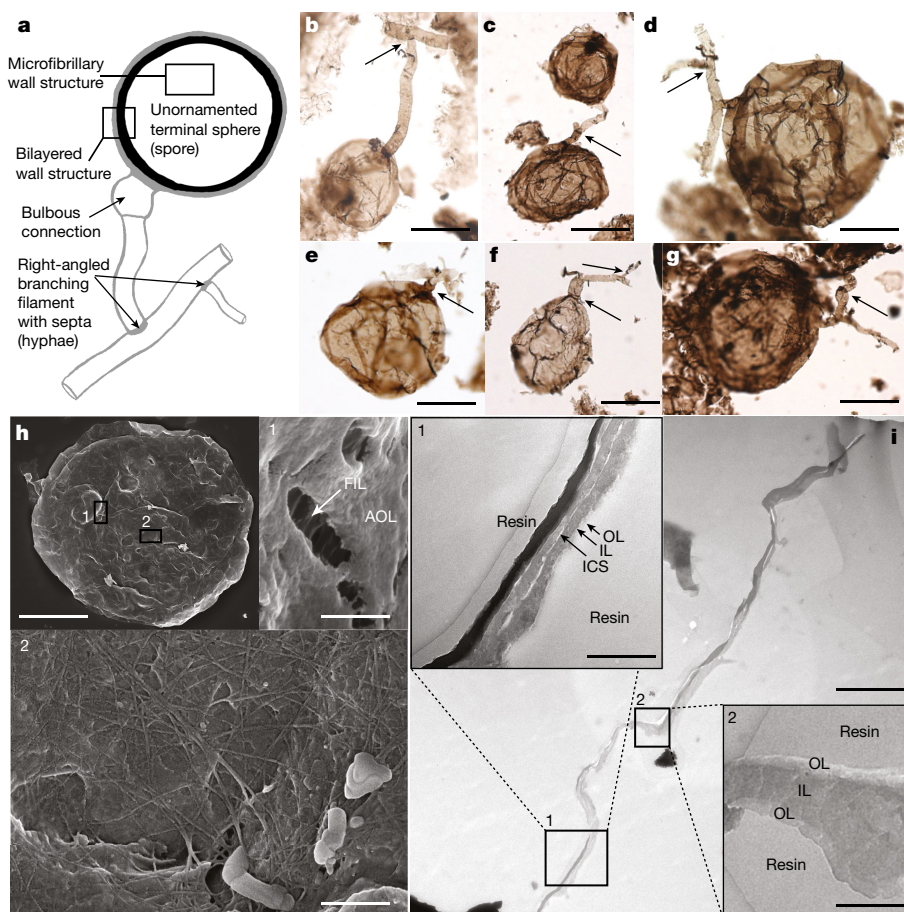


Fig. 1 | Microphotographs of *O. giraldae* specimens. **a**, Sketch of *O. giraldae*, displaying the main features of the microfossil. **b–h**, Unornamented terminal sphere (spore). **b–g**, Transmitted light microscopy images that show specimens with secondary branching at a right angle (**b**, **d–g**), with terminal spheres connected together (**c**), with a bulbous connection (**e**) and with tertiary branching (**d**, **f**, **g**). Arrows show septate connections. Details of sample and specimen numbers have previously been published¹⁴. **h**, SEM image shows the compressed vesicle. Inset 1 shows the two layers of the vesicle wall, with an amorphous outer layer (AOL) and a fibrillary inner layer (FIL). Inset 2 shows the intertwined microfibrils of the microfibrillary wall structure. **i**, TEM images show the compressed vesicles of the bilayer wall structure in ultra-thin section, with magnification in insets 1 and 2. The outer layer (OL), the inner layer (IL) and intracellular space (ICS) are indicated in both insets. Scale bars, 20 μm (**h**), 200 nm (**h** inset 1), 300 nm (**i** insets 1 and 2), 400 nm (**h** inset 2), 1,600 nm (**i**), 30 μm (**b–g**). Images **b–g** are modified from a previous publication¹⁴.

¹Early Life Traces & Evolution–Astrobiology Laboratory, UR Astrobiology, Geology Department, University of Liège, Liège, Belgium. ²Geological Survey of Canada, Ottawa, Ontario, Canada. ³Harquail School of Earth Sciences, Laurentian University, Sudbury, Ontario, Canada. ⁴UMR 7154 CNRS, Institut de Physique du Globe de Paris, Paris, France. *e-mail: c.loron@uliege.be; ej.javaux@uliege.be

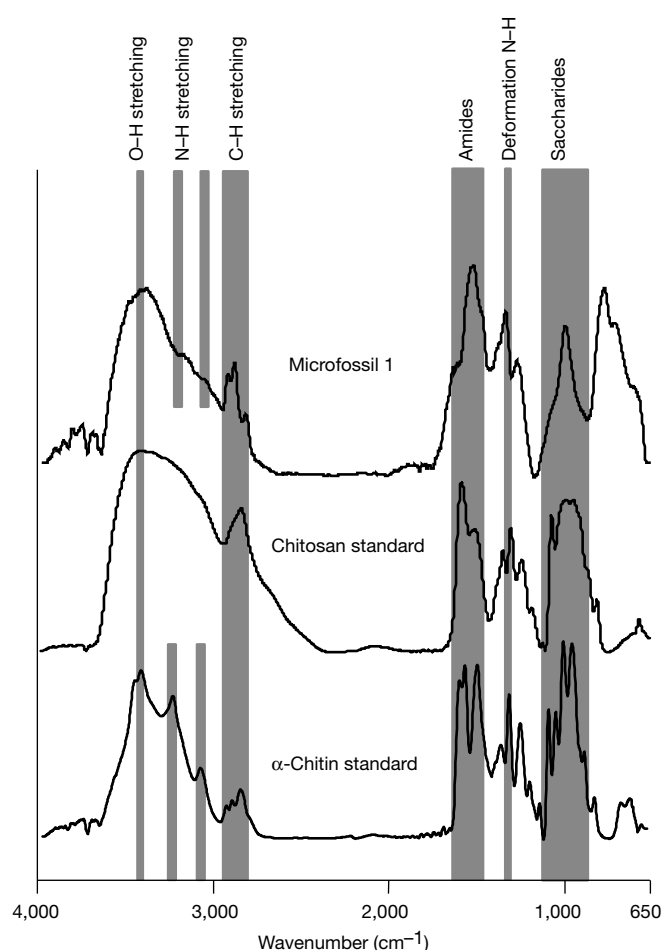


Fig. 2 | Spectra obtained with FTIR microspectroscopy. Representative spectra of one specimen (extracted microfossil 1) are compared to spectra of chitosan and α -chitin standards. Dark grey bands indicate the typical absorption bands of chitin and chitosan. The presence of spectral peaks for chitin and chitosan in *O. giraldae* supports its fungal affinity. See Supplementary Table 2 for band assignments. Each measurement was repeated three times with similar results.

Here we report abundant specimens of the organic-walled microfossil *Oursaphira giraldae*¹⁴, which are preserved parallel to lamination in shallow-water estuarine shale of the Grassy Bay Formation (Shaler Supergroup) from the Brock Inlier in the Northwest Territories of Canada^{15,16} (Extended Data Fig. 1). Uranium–lead dating of detrital zircon grains from the underlying Nelson Head Formation provide a maximum possible depositional date of $1,013 \pm 25$ million years ago (Ma) for the Grassy Bay Formation. Rhenium–osmium dating of organic matter in black shale from the overlying Boot Inlet Formation has yielded a date of 892 ± 13 Ma. These dates constrain the depositional date of the Grassy Bay Formation to between 1.0 and 0.9 billion years ago (Ga)^{17,18}.

The organic-walled microfossils consist of multicellular, branching, septate filaments with terminal spheres. Their resistance to the acid treatment used for mineral dissolution indicates a recalcitrant kerogenous composition, as confirmed by Raman microspectroscopy. Spheres are 33 to 80 μm in diameter ($n = 27$, $M = 54.3$, $\sigma = 13.6$) and are linked to the filaments (10 to 35 μm in length) by a single cylindrical or bulbous connection (Fig. 1a–g). Filament branching is right-angled, and up to three orders of branching are present (Fig. 1a–g). The connections between the spheres and the filaments—and between first-, second- and third-order branches—are septate (Fig. 1b–g).

Transmitted-light and scanning electron microscopy (SEM) examinations show smooth unornamented walls of filaments and spheres, although taphonomic pitting and localized degradation are present.

SEM images (secondary electron) also reveal the presence of locally well-preserved and intertwined (approximately 15–20-nm thick) microfibrils, which make up the walls (Fig. 1h, Extended Data Fig. 2). Ultrastructural analyses using transmission electron microscopy (TEM) show that the flattened microfossils are hollow, with a bilayered wall that consists of an electron-dense thick inner layer and a thin electron-tenuous outer layer (Fig. 1i).

This combination of complex morphology, right-angle branching, multicellularity, bilayered wall ultrastructure, compositional recalcitrance and relatively large size (not by itself a criterion) permits the unambiguous placement of the microfossil *O. giraldae* among eukaryotes; together they indicate the presence of a complex cytoskeleton, which is absent in prokaryotes¹⁹.

We performed Raman thermometry using Raman reflectance, which is an effective method for analysing low metamorphic-grade fossiliferous Proterozoic shale (see, for example, ref. ²⁰ and references therein). Average temperature estimates are approximately 195 °C (Supplementary Table 1). This low temperature is within the diagenesis window (<200 °C), which confirms that the rocks are not metamorphosed, consistent with the regional geology^{15,16} and with the quality of microfossil preservation. Analyses of extracted and in situ microfossils (in thin sections) produce similar estimates of temperature, which—as has previously been documented²⁰—indicates that extraction by acid maceration does not affect Raman analyses. This excellent preservation permits investigation of the molecular structure of the fossil wall using Fourier-transform infrared (FTIR) spectroscopy analyses. *O. giraldae* and the other microfossils from the same samples all exhibit a low degree of thermal alteration, consistent with the geological setting. This low degree of alteration—when combined with the microfossils being preserved flattened parallel to the shale laminations—demonstrates that the microfossils were deposited together and contemporaneously with sedimentation (syngenicity), rather than being a later contaminant.

To investigate the chemical composition of the wall, we performed FTIR spectroscopy on isolated microfossils. The spectra show absorption bands that are typical of chitin (*N*-acetyl-D-glucosamine) and/or chitosan (deacetylated D-glucosamine) (Fig. 2, Supplementary Table 2 and ref. ²¹). The typical absorption bands of cellulose are absent²².

The combination of the microfossil morphology, wall ultrastructure and chemistry of these microfossils is consistent with a fungal affinity. The septate filaments with right-angled branching and terminal spheres may be interpreted as hyphae with terminal spores, similar to the spore-bearing stages of many fungi^{4,7}. The relatively large size of the microfossils and their gross morphology bear some resemblance to fungal sporangia, but sphere opening or disintegration—which would indicate sporangial cleavage—is absent. A polarized growth and osmotrophic nutrition are characteristic of the Chytridiomycota, Blastocladiomycota and Dikarya (Ascomycota and Basidiomycota)²³. It is therefore possible that *O. giraldae* represents one of these clades. Septate hyphae are characteristic of the Dikarya, a few of the Zoopagomycota (such as the Kickxellales, in which the hyphae have a distinctive helicoidal morphology) and of the late stages of spores in the Mucoromycota, Chytridiomycota and Blastocladiomycota^{7,24,25}. Unlike in Dikarya, septa in the microfossil specimens are not regularly distributed along the hyphae; molecular clocks indicate a minimum date of 452 Ma for divergence of Dikarya⁶, much later than the rocks from which these fossils were obtained. These similarities and differences suggest that *O. giraldae* was probably in the stem Dikarya, or in a clade of the total fungi group that had some—but not all—of the characteristics of Dikarya.

Fungal walls are bilayered, as has been documented with TEM^{4,25} (Fig. 1i). The inner cell wall structure consists of intertwined microfibrils; these are locally well-preserved and visible in SEM images of the fossil material (Fig. 1h). The outer matrix—which is also visible in some of the fossil specimens (Fig. 1h, main panel and inset 1)—is composed mainly of chitin, glucan and proteins. In Dikarya, microfibrils are made of α -chitin and fixed by β -glucan, whereas in Mucoromycota the chitin

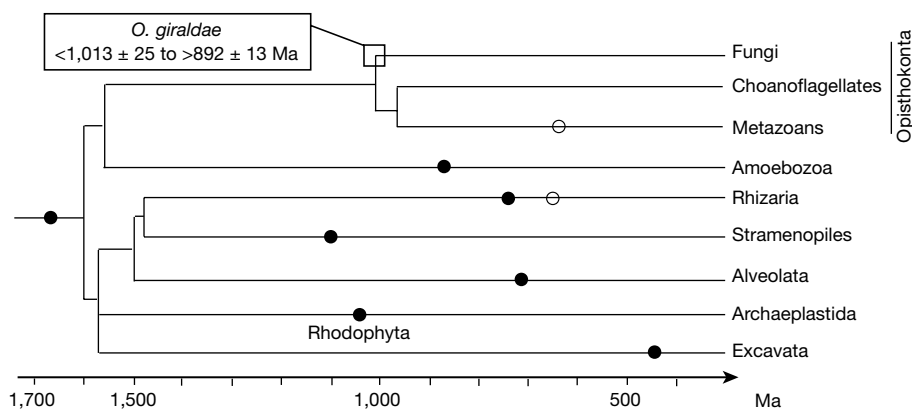


Fig. 3 | Simplified phylogenetic relationships of main eukaryotic supergroups. Diagram shows *O. giraldae* and its date range, and therefore the minimum date for the most recent common ancestor of fungi and the metazoan–choanoflagellate clade. The minimum dates for the appearance of each lineage are shown; these are based on either body fossil

occurrences (black dots) or molecular fossils (white dots). Details of dates, fossils and geological occurrences can be found in the Supplementary Information. Details about the relationships between the branches have previously been published⁹.

in the microfibrils is replaced by chitosan^{21,25}. Some of the life stages of pseudofungi (Oomycetes and Hyphochytridiomycetes) resemble the microfossils that we studied in terms of possessing local septa and branching, but have a low potential for preservation⁴. Although these pseudofungi may have chitin in their wall components²⁶, the major constituent of their walls is cellulose. Chitin synthesis may have evolved early in eukaryotes²⁷, and FTIR spectroscopy has proven efficient in detecting chitin and chitosan at temperatures²⁸ up to 280 °C. The presence of chitin and/or chitosan in our thermally immature specimens is therefore consistent with a fungal affinity.

Several multicellular micro- and macro-organisms (including pseudofungi, some life stages of xanthophyte algae, and slime moulds) are known to exhibit morphologies of ramified branching and terminal spheres that are broadly similar to the microfossils discussed here; however, the combination of morphology, wall ultrastructure, chitin and/or chitosan chemistry, and the absence of cellulose shown by the microfossils are most consistent with a fungal affinity^{4,7,25}. Other organisms that produce chitin (arthropods, chrysoflagellates, diatoms and ciliates) are morphologically very distinct from our specimens²⁹. In addition, a fungal affinity for these microfossils is consistent with molecular clock estimates for the early origin of fungi^{6,7}.

To date, the earliest uncontested fossil fungi are specimens from the 410-million-year-old Rhynie chert of Scotland⁴ and arbuscular spores of glomeromycotan fungi from Wisconsin that date to 450 Ma, in the Ordovician period⁵. These fossils have been used as the main calibration points for molecular-clock estimates that place the origin of fungi^{6,7} between 1,060 and 740 Ma—although this date may be older, depending on which calibrations are used for Dikarya³⁰. The 1–0.9-billion-year-old fossil fungi from the lower Shaler Supergroup reported here are older than these previously reported fossils by more than half a billion years, which provides a new calibration point for the evolution of fungi—and also for the evolution of the supergroup Opisthokonta, comprising fungi, metazoans and their protist relatives^{8,9} (Fig. 3).

As a consequence of their role in biological cycles (such as the degradation of organic matter, symbiosis and phosphate fixation), fungi today have key roles in aquatic and terrestrial ecosystem dynamics; they may have had similar roles in the Proterozoic era³. Fungi were also part of the early osmotrophic eukaryotic microbial community, which is documented from the Late Palaeoproterozoic or Early Mesoproterozoic eras^{10,31}. Extant fungi are mostly terrestrial, although some marine forms are known^{4,25}. Because *O. giraldae* is preserved in shallow-water estuarine shale of the Grassy Bay Formation, this fungus may have lived in an estuarine environment, in which the accumulation of organic detritus may have favoured fungal growth and heterotrophy; the fungus may also have been transported into this estuarine setting from land or marine niches.

The later colonization of terrestrial settings by fungi may have preceded and aided the colonization of land by plants through mycorrhizal symbioses and through soil processing, which would have provided ecological niches, improved the substrate, augmented nutrient uptake and increased aboveground productivity^{1,2}. As multidisciplinary studies of Proterozoic fossil assemblages progress, we predict that more fossil fungi and other early eukaryotes will be discovered and will improve our understanding of the evolution of the early biosphere.

Online content

Any methods, additional references, Nature Research reporting summaries, source data, statements of data availability and associated accession codes are available at <https://doi.org/10.1038/s41586-019-1217-0>.

Received: 23 January 2019; Accepted: 18 April 2019;

Published online 22 May 2019.

- Kenrick, P. & Crane, P. R. The origin and early evolution of plants on land. *Nature* **389**, 33–39 (1997).
- Jeffries, P., Gianinazzi, S., Perotto, S., Turnau, K. & Barea, J. M. The contribution of arbuscular mycorrhizal fungi in sustainable maintenance of plant health and soil fertility. *Biol. Fertil. Soils* **37**, 1–16 (2003).
- Berbee, M. L., James, T. Y. & Strullu-Derrien, C. Early diverging fungi: diversity and impact at the dawn of terrestrial life. *Annu. Rev. Microbiol.* **71**, 41–60 (2017).
- Taylor, T. N., Krings, M. & Taylor, E. L. *Fossil Fungi* (Academic, Amsterdam, 2014).
- Redecker, D., Kodner, R. & Graham, L. E. Glomalean fungi from the Ordovician. *Science* **289**, 1920–1921 (2000).
- Berbee, M. L. & Taylor, J. W. Dating the molecular clock in fungi—how close are we? *Fungal Biol. Rev.* **24**, 1–16 (2010).
- Watkinson, S. C., Boddy, L. & Money, N. *The Fungi* (Academic, London, 2015).
- Parfrey, L. W., Lahr, D. J., Knoll, A. H. & Katz, L. A. Estimating the timing of early eukaryotic diversification with multigene molecular clocks. *Proc. Natl Acad. Sci. USA* **108**, 13624–13629 (2011).
- Eme, L., Sharpe, S. C., Brown, M. W. & Roger, A. J. On the age of eukaryotes: evaluating evidence from fossils and molecular clocks. *Cold Spring Harb. Perspect. Biol.* **6**, a016139 (2014).
- Butterfield, N. J. Probable proterozoic fungi. *Paleobiology* **31**, 165–182 (2005).
- Retallack, G. J. Ediacaran life on land. *Nature* **493**, 89–92 (2013).
- Graham, L. E., Trest, M. T. & Cook, M. E. Acetolysis resistance of modern fungi: testing attributions of enigmatic Proterozoic and Early Paleozoic fossils. *Int. J. Plant Sci.* **178**, 330–339 (2017).
- Marshall, C. P., Javaux, E. J., Knoll, A. H. & Walter, M. R. Combined micro-Fourier transform infrared (FTIR) spectroscopy and micro-Raman spectroscopy of Proterozoic acritarchs: a new approach to palaeobiology. *Precamb. Res.* **138**, 208–224 (2005).
- Loron, C. C., Rainbird, R. H., Turner, E. C., Greenman, J. W. & Javaux, E. J. Organic-walled microfossils from the late Mesoproterozoic to early Neoproterozoic lower Shaler Supergroup (Arctic Canada): diversity and biostratigraphic significance. *Precamb. Res.* **321**, 349–374 (2019).
- Rainbird, R. H., Jefferson, C. W. & Young, G. M. The early Neoproterozoic sedimentary succession B of northwestern Laurentia: correlations and paleogeographic significance. *Geol. Soc. Am. Bull.* **108**, 454–470 (1996).
- Greenman, J. W. & Rainbird, R. H. *Stratigraphy of the Upper Nelson Head, Aok, Grassy Bay, and Boot Inlet Formations in the Brock Inlier, Northwest Territories (NTS*

- 97-A, D). Geological Survey of Canada Open File 8394 (Canada Geological Survey, Natural Resources Canada, 2018).
17. van Acken, D., Thomson, D., Rainbird, R. H. & Creaser, R. A. Constraining the depositional history of the Neoproterozoic Shaler Supergroup, Amundsen Basin, NW Canada: rhenium–osmium dating of black shales from the Wynnriatt and Boot Inlet Formations. *Precamb. Res.* **236**, 124–131 (2013).
 18. Rainbird, R. H. et al. Zircon provenance data record the lateral extent of pancontinental, early Neoproterozoic rivers and erosional unroofing history of the Grenville orogen. *Geol. Soc. Am. Bull.* **129**, 1408–1423 (2017).
 19. Javaux, E. J., Knoll, A. H. & Walter, M. Recognizing and interpreting the fossils of early eukaryotes. *Orig. Life Evol. Biosph.* **33**, 75–94 (2003).
 20. Baludikay, B. K. et al. Raman microspectroscopy, bitumen reflectance and illite crystallinity scale: comparison of different geothermometry methods on fossiliferous Proterozoic sedimentary basins (DR Congo, Mauritania and Australia). *Int. J. Coal Geol.* **191**, 80–94 (2018).
 21. Mohaček-Grošev, V., Božac, R. & Puppels, G. J. Vibrational spectroscopic characterization of wild growing mushrooms and toadstools. *Spectrochim. Acta A* **57**, 2815–2829 (2001).
 22. Kačuráková, M., Capek, P., Sasinková, V., Wellner, N. & Ebringerová, A. FT-IR study of plant cell wall model compounds: pectic polysaccharides and hemicelluloses. *Carbohydr. Polym.* **43**, 195–203 (2000).
 23. Riquelme, M. & Sánchez-León, E. The Spitzenkörper: a choreographer of fungal growth and morphogenesis. *Curr. Opin. Microbiol.* **20**, 27–33 (2014).
 24. Spatafora, J. W. et al. A phylum-level phylogenetic classification of zygomycete fungi based on genome-scale data. *Mycologia* **108**, 1028–1046 (2016).
 25. Webster, J. & Weber, R. *Introduction to Fungi* (Cambridge Univ. Press, Cambridge, 2007).
 26. Mérida, H., Sandoval-Sierra, J. V., Diéguez-Uribeondo, J. & Bulone, V. Analyses of extracellular carbohydrates in oomycetes unveil the existence of three different cell wall types. *Eukaryot. Cell* **12**, 194–203 (2013).
 27. Richards, T. A., Leonard, G. & Wideman, J. G. What defines the “kingdom” fungi? *Microbiol. Spectr.* **5**, FUNK-0044-2017 (2017).
 28. Wanjun, T., Cunxin, W. & Donghua, C. Kinetic studies on the pyrolysis of chitin and chitosan. *Polym. Degrad. Stabil.* **87**, 389–394 (2005).
 29. Muzzarelli, R. A. A. in *Chitin: Formation and Diagenesis (Topics in Geobiology Vol. 34)* (ed. Gupta, N. S.) 1–34 (Springer Science and Business Media, New York, 2010).
 30. Taylor, J. W. & Berbee, M. L. Dating divergences in the fungal tree of life: review and new analyses. *Mycologia* **98**, 838–849 (2006).
 31. Javaux, E. J. & Knoll, A. H. Micropaleontology of the lower Mesoproterozoic Roper Group, Australia, and implications for early eukaryotic evolution. *J. Paleontol.* **91**, 199–229 (2017).

Acknowledgements This research was supported by the Agouron Institute, the FRS-FNRS-FWO EOS ET-Home grant 30442502 and the ERC Stg ELITE FP7/308074. We thank M. Giraldo, M.-C. Sforna, Y. Cornet and S. Smeets (University of Liège) for technical support and the Geological Survey of Canada’s Geomapping for Energy and Minerals Program for fieldwork logistics.

Reviewer information *Nature* thanks Linda Graham and the other anonymous reviewer(s) for their contribution to the peer review of this work.

Author contributions C.C.L. and E.J.J. conceived the study and interpreted the data. C.F. and C.C.L. performed the Raman and FTIR analyses. C.C.L., C.F. and S.B. performed the TEM and SEM sample preparation and observations. R.H.R. and E.C.T. sampled the rocks and collected the geological data. C.C.L. and E.J.J. wrote the paper with contribution from all the authors. E.J.J. supervised the project.

Competing interests The authors declare no competing interests.

Additional information

Extended data is available for this paper at <https://doi.org/10.1038/s41586-019-1217-0>.

Supplementary information is available for this paper at <https://doi.org/10.1038/s41586-019-1217-0>.

Reprints and permissions information is available at <http://www.nature.com/reprints>.

Correspondence and requests for materials should be addressed to C.C.L. or E.J.J.

Publisher’s note: Springer Nature remains neutral with regard to jurisdictional claims in published maps and institutional affiliations.

© The Author(s), under exclusive licence to Springer Nature Limited 2019

METHODS

Sample preparation. The shale sample 15RAT-021A1 (Grassy Bay Formation, Shaler Supergroup, Canada) was cut into thin sections parallel to lamination for the Raman analyses. A fraction of the sample was demineralized by treatment with HF and HCl, using a previously published method³², without centrifugation to minimize mechanical shocks. A part of the residue was mounted on microscopic slides. Single microfossils were hand-picked under an inverted microscope with a micropipette, and deposited on a glass slide and ZnSe disc for spectroscopic analyses.

Optical microscopy. Optical microscopy was performed on a Zeiss Axio imager microscope equipped with an Axiocam MRc5. Measurements were taken using the software AxioVision.

SEM. SEM analyses were performed using an Auriga 40 Field Emission Gun Scanning Electron Microscope (FEG SEM) Zeiss, at the electron microscopy platform of the Institut de Physique du Globe de Paris (Platform PARI). The images were taken using the Secondary Electron Detector InLens and/or Everhart Thornley at 15-keV accelerating voltage, with a beam current at 800 pA and a working distance between 2.5 and 7.5 mm. Analyses were performed on specimens deposited on glass slides, and Au-coated with a Quorum Q150 ES metallizer.

TEM. Isolated microfossils were embedded in agar-agar gelose and dehydrated in a graded ethanol series, then infiltrated successively in 1,2-propylene oxide, 1:1 propylene oxide/epoxy resin melange and then in pure epoxy resin. The samples were placed in silicon moulds and left to polymerize at 60 °C for 3 days. The resin blocks were cut into ultrathin (60–100 nm) transversal sections with a diamond knife on an ultramicrotome Reichert Ultracut. Sections were put on formvar-coated copper grids and imaged at an accelerating voltage of 200 kV with a transmission electron microscope Tecnai G² Twin (CAREM, University of Liège).

Raman microspectroscopy. Raman spectra were collected on polished thin sections and on isolated microfossils using a Renishaw INVIA Raman microspectrometer, at the 'Early Life Traces and Evolution–Astrobiology Laboratory' (UR Astrobiology, Geology Department, University of Liège) (see Supplementary Information). Raman analyses were done using an Ar-ion, 40-mW monochromatic 514-nm laser source. Laser excitation was focused through a 50× objective to obtain a 1–2- μm spot size. The Raman spectrum of each point (around 20 points were measured for each specimen) was acquired in static mode (fixed at a wavenumber of 1,150 cm^{-1}) for 1 \times 1-s running time. This enabled the acquisition of Raman spectra with a 2,000- cm^{-1} detection range and a 4- cm^{-1} spectral resolution. To process the data, we used the software 'Renishaw Wire 4.1'. The baseline subtraction protocol was performed on a truncated spectrum between 1,000 and 1,800 cm^{-1} , with a third-order polynomial fit. Data processing followed a previously published protocol³³. Thermal maturity of carbonaceous material was assessed following a previously published protocol²⁰, using the Raman reflectance parameter (RmcR0%), which is an equivalent of vitrinite reflectance (vR0%)^{34,35}. The RmcR0% parameter uses the positions (ω) of the D1 and G peaks, and is defined as $\text{RmcR0\%} \equiv \text{vR0 eq\%} = 0.0537 \times (\omega\text{G} - \omega\text{D1}) - 11.21$ (see ref. ³⁴).

The Raman reflectance method appears to be a robust tool for evaluating the thermal maturity of carbonaceous material from Proterozoic rocks²⁰.

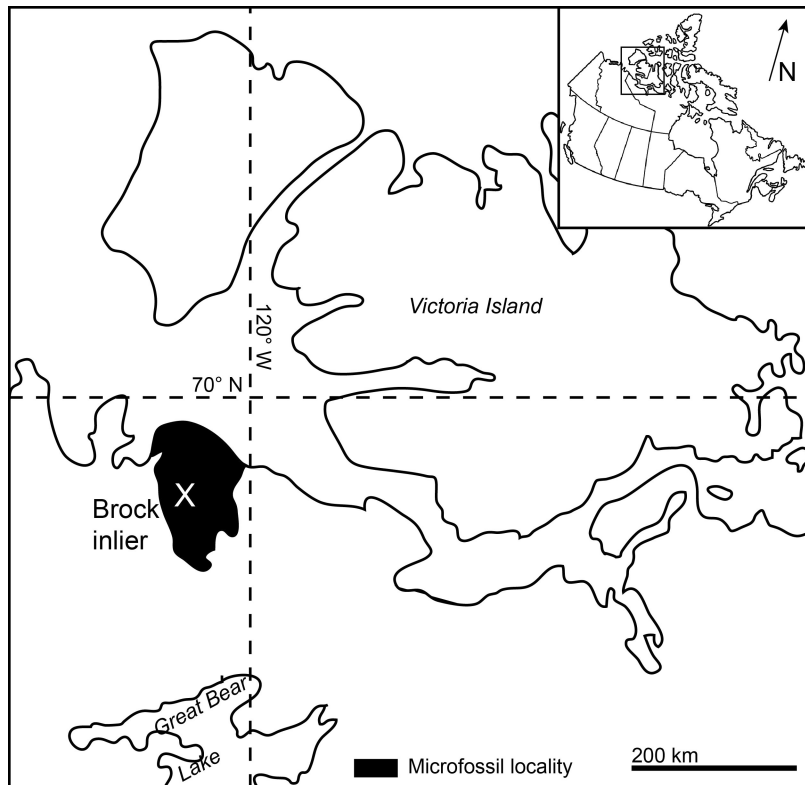
FTIR microspectroscopy. The analyses were performed with a Hyperion 2000 Bruker microscope coupled to a Tensor 27 FTIR spectrometer at the Early Life Traces and Evolution–Astrobiology Laboratory. The specimens were pipetted out of Milli-Q water and deposited on ZnSe plates. Data were collected with a conventional Globar source equipped with 15× objective (NA = 0.4) and a liquid-nitrogen-cooled MCT-A detector. Background was collected on a ZnSe plate free of sample, by combining 32 accumulations. Thirty-two scans were accumulated in transmission mode from each specimen with a spectral range that spanned between 650 cm^{-1} and 4,000 cm^{-1} , with a resolution of 4 cm^{-1} . The spectra were treated, atmospheric water and CO₂ were removed and the baseline corrected, using the software 'Opus 8.0'. Standards for chitin (shrimp shells, Sigma, C7170-100G) and chitosan (shrimp shells, $\geq 75\%$; Sigma-Aldrich, C3646-10G) were each deposited on ZnSe plates. Spectra were acquired with the same parameters as those used for the microfossil analyses. Band assignments of the spectra are based on previous studies^{21,36–39} (see also Supplementary Table 2).

Reporting summary. Further information on research design is available in the Nature Research Reporting Summary linked to this paper.

Data availability

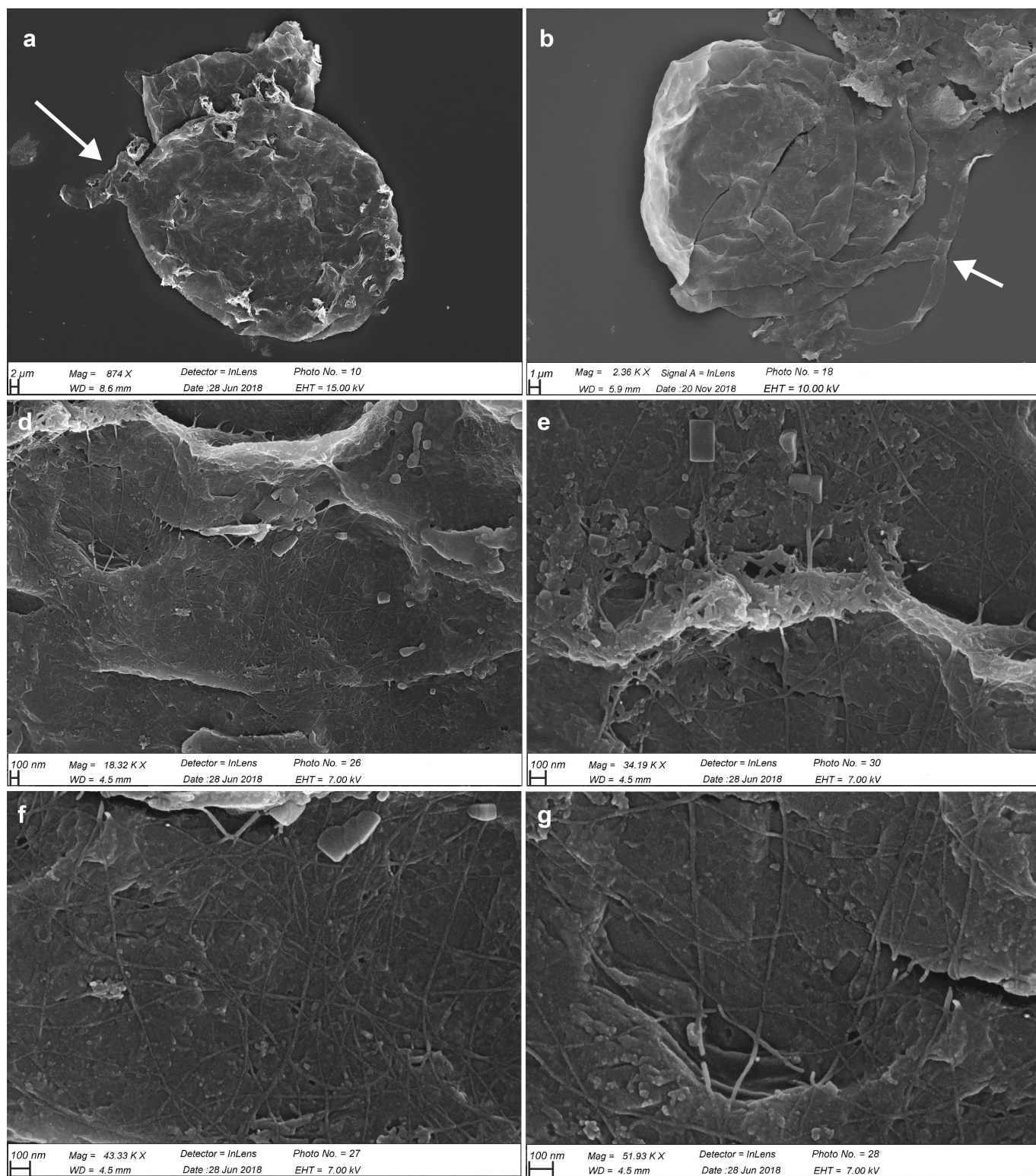
All processed data are included in Supplementary Tables 1 and 2. Raw data are available from the corresponding authors upon reasonable request. Microfossil specimens are accessible at the Early Life Traces and Evolution–Astrobiology Laboratory.

- Grey, K. A *Modified Palynological Preparation Technique for the Extraction of Large Neoproterozoic Acanthomorph Acritarchs and Other Acid-Soluble Microfossils*. (Geological Survey of Western Australian, Department of Minerals and Energy, Perth, 1999).
- Sforna, M. C., Van Zuilen, M. A. & Philippot, P. Structural characterization by Raman hyperspectral mapping of organic carbon in the 3.46 billion-year-old Apex chert, Western Australia. *Geochim. Cosmochim. Acta* **124**, 18–33 (2014).
- Liu, D. H. et al. Sample maturation calculated using Raman spectroscopic parameters for solid organics: methodology and geological applications. *Chin. Sci. Bull.* **58**, 1285–1298 (2013).
- Sauerer, B., Craddock, P. R., AlJohani, M. D., Alsamadony, K. L. & Abdallah, W. Fast and accurate shale maturity determination by Raman spectroscopy measurement with minimal sample preparation. *Int. J. Coal Geol.* **173**, 150–157 (2017).
- Paulino, A. T., Simionato, J. I., Garcia, J. C. & Nozaki, J. Characterization of chitosan and chitin produced from silkworm crysalides. *Carbohydr. Polym.* **64**, 98–103 (2006).
- Movasaghi, Z., Rehman, S. & Rehman, D. I. Fourier transform infrared (FTIR) spectroscopy of biological tissues. *Appl. Spectrosc. Rev.* **43**, 134–179 (2008).
- Michell, A. J. & Scurfield, G. Composition of extracted fungal cell walls as indicated by infrared spectroscopy. *Arch. Biochem. Biophys.* **120**, 628–637 (1967).
- Bahmed, K., Quilès, F., Bonaly, R. & Coulon, J. Fluorescence and infrared spectrometric study of cell walls from *Candida*, *Kluyveromyces*, *Rhodotorula* and *Schizosaccharomyces* yeasts in relation with their chemical composition. *Biomacromolecules* **4**, 1763–1772 (2003).

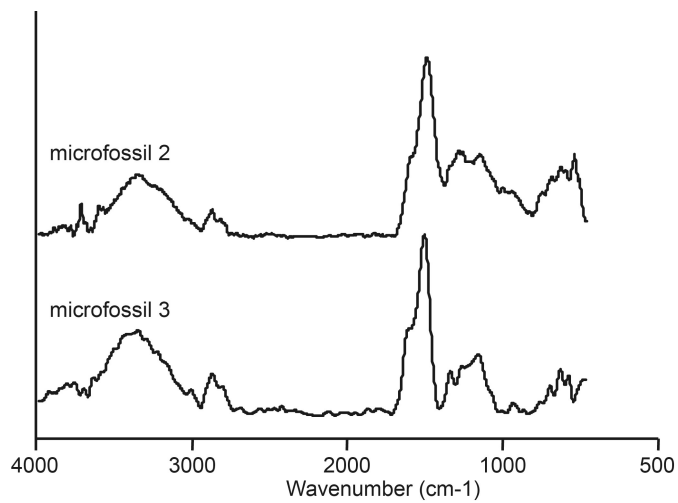


Extended Data Fig. 1 | Location of the study area in northwestern Canada, highlighting the Brock Inlier. The white cross indicates the location at which the samples were extracted ($68^{\circ} 55' 42''$ N,

$121^{\circ} 44' 17''$ W). The stratigraphic column and geology have previously been published¹⁴⁻¹⁶. The map is modified after a previous publication¹⁴.



Extended Data Fig. 2 | Additional SEM images. a, b, *O. giraldae* (whole specimen) with right-angled branching hyphae (indicated with arrows). d–g, Detailed images of microfibrils on the surface of the specimen shown in Fig. 1h.



Extended Data Fig. 3 | Additional spectra of *O. giraldae*, showing a more-advanced state of degradation. The typical peaks of chitin and chitosan are present, but at a lower intensity than in the standard. The region of the saccharides (wavenumber of 1,200–800 cm⁻¹), which is necessary for polymer recognition, is very weak in intensity. Each measurement was repeated three times with similar results.

Reporting Summary

Nature Research wishes to improve the reproducibility of the work that we publish. This form provides structure for consistency and transparency in reporting. For further information on Nature Research policies, see [Authors & Referees](#) and the [Editorial Policy Checklist](#).

Statistics

For all statistical analyses, confirm that the following items are present in the figure legend, table legend, main text, or Methods section.

n/a Confirmed

- The exact sample size (n) for each experimental group/condition, given as a discrete number and unit of measurement
- A statement on whether measurements were taken from distinct samples or whether the same sample was measured repeatedly
- The statistical test(s) used AND whether they are one- or two-sided
Only common tests should be described solely by name; describe more complex techniques in the Methods section.
- A description of all covariates tested
- A description of any assumptions or corrections, such as tests of normality and adjustment for multiple comparisons
- A full description of the statistical parameters including central tendency (e.g. means) or other basic estimates (e.g. regression coefficient) AND variation (e.g. standard deviation) or associated estimates of uncertainty (e.g. confidence intervals)
- For null hypothesis testing, the test statistic (e.g. F , t , r) with confidence intervals, effect sizes, degrees of freedom and P value noted
Give P values as exact values whenever suitable.
- For Bayesian analysis, information on the choice of priors and Markov chain Monte Carlo settings
- For hierarchical and complex designs, identification of the appropriate level for tests and full reporting of outcomes
- Estimates of effect sizes (e.g. Cohen's d , Pearson's r), indicating how they were calculated

Our web collection on [statistics for biologists](#) contains articles on many of the points above.

Software and code

Policy information about [availability of computer code](#)

Data collection AxioVision SE64 Rel. 4.9.1 software, Opus 8.0 software, Renishaw Wire 4.1 software

Data analysis Opus 8.0 software, Renishaw Wire 4.1 software

For manuscripts utilizing custom algorithms or software that are central to the research but not yet described in published literature, software must be made available to editors/reviewers. We strongly encourage code deposition in a community repository (e.g. GitHub). See the Nature Research [guidelines for submitting code & software](#) for further information.

Data

Policy information about [availability of data](#)

All manuscripts must include a [data availability statement](#). This statement should provide the following information, where applicable:

- Accession codes, unique identifiers, or web links for publicly available datasets
- A list of figures that have associated raw data
- A description of any restrictions on data availability

All processed data are included in Supplementary Material Table I and II. Raw data are available from the corresponding author upon reasonable request. Microfossils specimens are accessible in the collections of the "Early Life Traces and Evolution" Laboratory, Geology department, University of Liège, Belgium.

Field-specific reporting

Please select the one below that is the best fit for your research. If you are not sure, read the appropriate sections before making your selection.

- Life sciences Behavioural & social sciences Ecological, evolutionary & environmental sciences

Ecological, evolutionary & environmental sciences study design

All studies must disclose on these points even when the disclosure is negative.

Study description	morphological, ultrastructural and microchemical analyses of organic-walled microfossils
Research sample	A fossil population of <i>Ourasphaera giraldae</i> from one bed of Grassy Bay Formation, Shaler Supergroup, Arctic Canada. The sample was chosen for its very good preservation and the abundance of microfossil specimens.
Sampling strategy	We selected the best and complete specimens from the <i>Ourasphaera giraldae</i> population.
Data collection	C.C.L. and E.J.J. conceived the study and interpreted the data. C.F. and C.C.L performed the RAMAN and FTIR analyses. C.C.L., C.F. and S.B. performed the TEM/SEM sample preparation and observations. R.H.R and E.C.T. sampled the rocks and collected the geological data. C.C.L and E.J.J. wrote the paper with contribution of all the authors. E.J.J. supervised the project.
Timing and spatial scale	Analyses of microfossils were conducted during the year 2018
Data exclusions	no data have been excluded
Reproducibility	27 microfossils were measured, 6 specimens were prepared for TEM, 5 specimens for SEM, 2 specimens for RAMAN (in thin section and extracted) and 3 specimens were prepared for FTIR microspectroscopy
Randomization	This is not relevant for our study because the studied microfossils represent one taxon
Blinding	This is not relevant for our study because the studied microfossils represent one taxon
Did the study involve field work?	<input type="checkbox"/> Yes <input checked="" type="checkbox"/> No

Reporting for specific materials, systems and methods

We require information from authors about some types of materials, experimental systems and methods used in many studies. Here, indicate whether each material, system or method listed is relevant to your study. If you are not sure if a list item applies to your research, read the appropriate section before selecting a response.

Materials & experimental systems

n/a	Involved in the study
<input checked="" type="checkbox"/>	<input type="checkbox"/> Antibodies
<input checked="" type="checkbox"/>	<input type="checkbox"/> Eukaryotic cell lines
<input type="checkbox"/>	<input checked="" type="checkbox"/> Palaeontology
<input checked="" type="checkbox"/>	<input type="checkbox"/> Animals and other organisms
<input checked="" type="checkbox"/>	<input type="checkbox"/> Human research participants
<input checked="" type="checkbox"/>	<input type="checkbox"/> Clinical data

Methods

n/a	Involved in the study
<input checked="" type="checkbox"/>	<input type="checkbox"/> ChIP-seq
<input checked="" type="checkbox"/>	<input type="checkbox"/> Flow cytometry
<input checked="" type="checkbox"/>	<input type="checkbox"/> MRI-based neuroimaging

Palaeontology

Specimen provenance	Fraction of rock sample from one bed of Grassy Bay Formation, Shaler Supergroup, Arctic Canada, collected by R.H.R and E.C.T in Canada with the support the Geological Survey of Canada, stored in the collection of the "Early Life Traces and Evolution" Laboratory", UR Astrobiology, Geology Department of the University of Liège, Belgium
Specimen deposition	the microscopic slides are stored in the collection of the "Early Life Traces and Evolution" Laboratory", UR Astrobiology, Geology Department of the University of Liège, Belgium
Dating methods	No new dates are provided
<input checked="" type="checkbox"/> Tick this box to confirm that the raw and calibrated dates are available in the paper or in Supplementary Information.	